Cryptococcus neoformans Requires a Functional Glycolytic Pathway for Disease but Not Persistence in the Host

Michael S. Price,[a] Marisol Betancourt-Quiroz,[a] Jennifer L. Price,[a]* Dena L. Toffaletti,[a] Haily Vora,[a] Guanggan Hu,[b] James W. Kronstad,[b] and John R. Perfect[a]

Department of Medicine, Duke University Medical Center, Durham, North Carolina, USA,[a] and The Michael Smith Laboratories, The University of British Columbia, Vancouver, British Columbia, Canada[b]

* Present address: Beckman Coulter Genomics, Morrisville, North Carolina, USA.

ABSTRACT ***Cryptococcus neoformans* is an important fungal pathogen of immunocompromised individuals, with a close relative, *Cryptococcus gattii*, emerging as a serious threat for the immunocompetent. During initial infection, *C. neoformans* colonizes the airspaces of the lungs, resulting in pneumonia, and subsequently migrates to the central nervous system (CNS). We sought to understand fungal carbon utilization during colonization of these fundamentally different niches within the host, in particular the roles of gluconeogenesis and glycolysis. We created mutants at key points in the gluconeogenesis/glycolysis metabolic pathways that are restricted for growth on lactate and glucose, respectively. A phosphoenolpyruvate carboxykinase mutant (the *pck1*Δ mutant), blocked for entry of 2- and 3-carbon substrates into gluconeogenesis and attenuated for virulence in a murine inhalation model, showed wild-type (WT) persistence in a rabbit cerebrospinal fluid (CSF) model of cryptococcosis. Conversely, both the pyruvate kinase (*pyk1*Δ) and the hexose kinase I and II (*hxk1*Δ/*hxk2*Δ) mutants, which show impaired glucose utilization, exhibited severely attenuated virulence in the murine inhalation model of cryptococcosis and decreased persistence in the CNS in both the rabbit CSF and the murine inhalation models while displaying adequate persistence in the lungs of mice. These data suggest that glucose utilization is critical for virulence of C. *neoformans* and persistence of the yeast in the CNS.**

IMPORTANCE ***Cryptococcus neoformans* is an emerging fungal pathogen of humans and is responsible for approximately 625,000 deaths annually among those suffering from HIV infection/AIDS. The ability of this fungus to persist in the host, coupled with its propensity to colonize the CNS, makes the understanding of nutrient acquisition in the host a primary concern. In this study, we report a requirement of glucose utilization for virulence of *C. neoformans* that is separate from its role in ATP production in the pathogen. Furthermore, we show that inhibition of glycolysis is a viable antifungal drug target, and impaired ATP production via the *PYK1* deletion may serve as a model for dormant/chronic fungal infection in the host. Taken together, these results demonstrate the critical importance of understanding basic metabolic processes of the fungus in the context of host-pathogen interactions.**

Received 11 May 2011 **Accepted** 17 May 2011 **Published** 7 June 2011

Citation Price MS, et al. 2011. *Cryptococcus neoformans* requires a functional glycolytic pathway for disease but not persistence in the host. mBio 2(3):e00103-11. doi:10.1128/mBio.00103-11.

Editor Françoise Dromer, Institut Pasteur

Address correspondence to John R. Perfect, perfe001@mc.duke.edu.

Cryptococcus neoformans is a major human and animal pathogen responsible for cryptococcal meningoencephalitis in immunocompromised individuals. Found worldwide, *C. neoformans* is commonly isolated from environmental samples (1). Cryptococcosis is currently the third highest cause of mortality due to infectious diseases in sub-Saharan Africa (2), and an ongoing outbreak of *Cryptococcus gattii* infections is causing measurable human and animal morbidity and mortality in the Pacific Northwest (3–5). Unlike many other opportunistic fungal pathogens (e.g., *Aspergillus fumigatus*), *C. neoformans* appears to be specially adapted for survival in the human host and possesses a number of pathogenicity factors involved in this interaction (6). However, this pathogen does not appear to be part of the normal human flora, despite its intimate association with monocytes and the central nervous system (CNS) during disease (7–12).

Several virulence-associated traits have clearly been identified as required for cryptococcal pathogenesis, including growth at 37°C, production of capsule, melanin biosynthesis, secretion of phospholipase, and production of mannitol (13, 14). The polysaccharide capsule has received much attention due to its immunomodulatory properties (12) and is mainly composed of GXM (α1,3-linked mannose subunits with various xylosyl and β-glucuronyl substitutions), which varies by serotype. Interestingly, elimination of individual sugar components (e.g., xylose) results in virulence defects (15). Therefore, understanding the process of carbon assimilation by *C. neoformans* and therefore subsequent capsule biosynthesis is crucial for a proper understanding of virulence.

Recently, Barelle and colleagues demonstrated that the ascomycete yeast pathogen *Candida albicans* alters its carbon assimi-

lation from nonfermentative (i.e., gluconeogenesis and glyoxylate cycle) to fermentative (i.e., glycolysis) metabolism during the onset of systemic infection in mice (16). In their study, they built upon previous studies showing the seemingly paradoxical importance of both fermentative and nonfermentative carbon metabolism in *C. albicans* virulence (17–19). Using mutants blocked in various core carbon metabolic pathways, Barelle and colleagues showed that the glyoxylate cycle and gluconeogenesis pathways were essential for optimal survival of *C. albicans* during its initial interactions with immune cells (16). Later, as the yeast cells colonize the bloodstream and internal organs of the mammalian host, glycolysis emerges as the main carbon assimilation pathway. This study emphasized the changes in carbon assimilation a pathogen must make to persist in spite of changing host defenses.

Presumably, C. *neoformans* also encounters several fundamentally different microenvironments in the host during the course of disease progression. For instance, we recently demonstrated that persistence of *C. neoformans* in the cerebrospinal fluid (CSF) microenvironment was influenced by a number of different cellular pathways, including maintenance of ionic balance and inositol metabolism (20). Previous studies touching on carbon metabolism and *C. neoformans* pathogenesis show mixed results regarding the role of nonpreferred carbon sources in disease progression (21–24). However, nonpreferred carbon sources such as lactate and acetate are likely important early in establishment of a pulmonary infection. For example, the acetyl-coenzyme A (CoA) synthase gene *ACS1* has been demonstrated as necessary for full virulence in *C. neoformans* (21). In this same study, Hu and colleagues showed that Snf1, shown to be a major regulator of nonpreferred carbon utilization via the phosphorylation of the global carbon catabolite repressor Mig1 in *Saccharomyces cerevisiae*, is also required for full virulence in a murine inhalation model of cryptococcosis. However, there are differences between *C. neoformans* and other pathogenic fungi in the relationship of carbon utilization and virulence. For example, the glyoxylate shunt is not required for virulence in this basidiomycete pathogen as it is for the full virulence of the ascomycete *C. albicans* (18, 22, 24).

The ability of a pathogen to cause disease is inextricably linked to its ability to procure nutrients from its host, and carbon in particular. Therefore, a solid understanding of carbon acquisition by a microbial invader or tumor cell is essential for identifying potential targets for the development of drug therapies. This line of reasoning is currently being employed with regard to cancer treatment. Cancer cells are known to exhibit differential carbon metabolism compared to normal host tissue (25). For instance, malignant cells switch on proliferative carbon metabolism dependent on glycolysis for the production of their biomass, making them vulnerable to inhibitors of glycolysis (26). The apparent similarities observed between malignancies and eukaryotic microorganisms regarding carbon metabolism during host invasion (25) warrants further investigation of carbon metabolism during infection for unique weaknesses that can be targeted in treatment strategies for pathogenic fungi such as *C. neoformans*.

Therefore, we sought to understand the relationship of glucose anabolic and catabolic processes to pathogenicity in C. *neoformans*. To investigate the roles of glycolysis and gluconeogenesis in host colonization by *Cryptococcus*, we procured carbon metabolism mutants previously described as well as constructed additional mutants to block key steps in glycolysis/gluconeogenesis and carbon catabolite repression (CCR) (see Table S1 and Fig. S1 in the supplemental material) (21, 22). By examining the effects of these mutations on virulence at several body sites using both the murine inhalation (pulmonary infection and dissemination) and the rabbit CSF (direct inoculation of the subarachnoid space) models of cryptococcosis, we demonstrate that gluconeogenic carbon assimilation is sufficient for the initial establishment of infection but that glycolysis is critical for persistence of *C. neoformans* in the CNS and virulence in the host.

RESULTS

Role of gluconeogenesis in *C. neoformans* persistence in the CNS. Since prior reports have demonstrated the importance of gluconeogenesis during lung infection by *C. neoformans*, we sought to establish a possible role for gluconeogenesis in survival of *C. neoformans* in the CNS. We used real-time PCR to measure expression of the phosphoenolpyruvate carboxykinase gene *PCK1*, which encodes the main gateway enzyme for entry of 2- and 3-carbon substrates into gluconeogenesis, under different growth conditions. We confirmed elevated *PCK1* expression in low glucose concentrations, as expected from results obtained using *S. cerevisiae* (27), and also observed increased expression due to exposure to *ex vivo* pooled human CSF (Fig. 1A). This increased *PCK1* expression in strain H99 was also observed *in vivo* in the rabbit CSF model of cryptococcosis and in cryptococcal strains taken directly from human patient CSF samples compared to the expression of *PCK1* in these samples grown *in vitro* at 37°C (Fig. 1B and C). However, despite this elevated expression of *PCK1*, independent *pck1*Δ deletion mutants showed no defects in CNS persistence or viability in the rabbit CSF model (data not shown).

We also tested other previously published mutants related to nonpreferred carbon assimilation in the rabbit CSF model. A *snf1*Δ deletion mutant, which is thought to represent a major regulator of nonpreferred carbon utilization based on findings in *S. cerevisiae*, demonstrated moderately reduced persistence in the rabbit CSF model (Fig. 1D). The *snf1*Δ mutant exhibits increased sensitivity to sodium nitrite, decreased melanin production, and growth on acetate as a sole carbon source at 37°C and is avirulent in the murine inhalation model (21). Furthermore, a recent study using a serotype D strain of *C. neoformans* has also shown that *SNF1* deletion impairs growth at 39°C, which is the normal body temperature for rabbits (28). Therefore, we also tested a major pathway for 2-carbon utilization via the tricarboxylic acid (TCA) cycle. *ACS1* encodes acetyl-CoA synthase, and the *acs1*Δ mutant fails to grow on 2-carbon substrates and exhibits modestly attenuated virulence in the murine-inhalational model of cryptococcosis (21). However, the *acs1*Δ mutant showed no defects in CNS persistence in the rabbit CSF model (Fig. 1D). Taken together, these data regarding *PCK1*, *SNF1*, and *ACS1* support the hypothesis that carbon assimilation by *C. neoformans* for disease production and yeast persistence in the CNS is likely via glycolysis.

Pyruvate kinase is required for *C. neoformans* pathogenesis but not persistence in the lung. Since blocked entry of 2- and 3-carbon compounds into gluconeogenesis by deletion of *ACS1* or *PCK1* showed no adverse effect on persistence of *C. neoformans* in the CNS, we sought to define the specific role of glycolysis in persistence of the fungus in the CNS. Therefore, we blocked the exit of carbon from glycolysis via the deletion of the pyruvate kinase homolog *PYK1*. As expected, the *pyk1*Δ mutant strain was unable to grow on glucose, fructose, ribose, or glycerol but was viable on either acetate or lactate as a sole carbon source (see

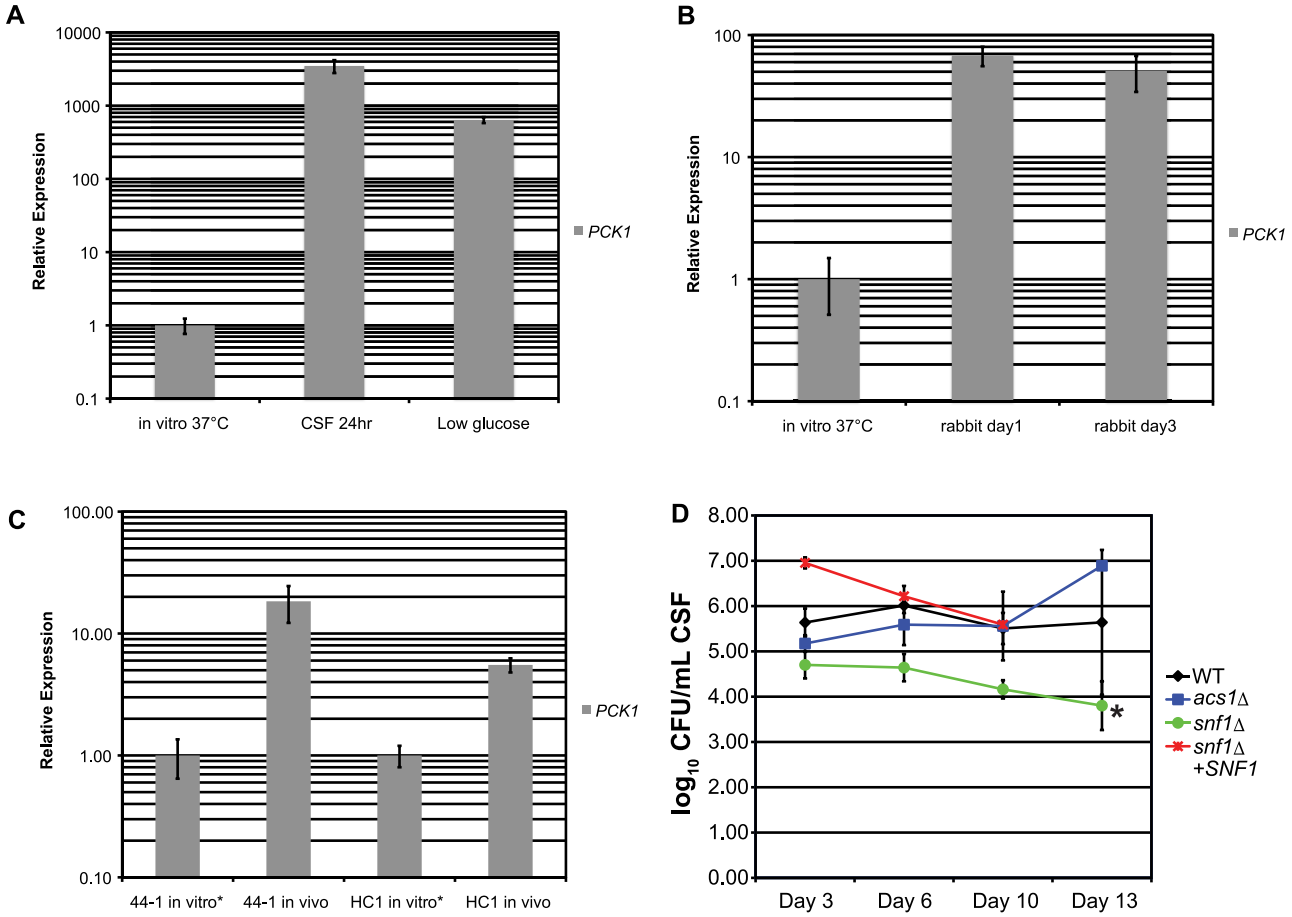

FIG 1 *PCK1* expression does not correlate with CNS persistence of *C. neoformans*. (A) *PCK1* expression was measured by real-time PCR following exposure to either CSF or YNB-0.05% glucose (low glucose) for 24 h at 37°C. *PCK1* expression following growth in YPD at 37°C (*in vitro* 37°C) was used as a positive control. (B) *PCK1* expression in *C. neoformans* was measured by real-time PCR during rabbit infection. Expression levels *in vivo* were compared to those from yeast grown in YPD at 37°C (*in vitro* 37°C). (C) *PCK1* expression levels were measured by real-time PCR for *C. neoformans* isolated from human CSF samples. *C. neoformans* strains 44-1 and HC1 were obtained from the Duke University Infectious Disease Specimen Repository, which houses specimens isolated from deidentified patients with cryptococcal meningitis. *PCK1* transcripts for *C. neoformans* cultured from the CSF samples and grown in YPD at 37°C ("in vitro" samples) were compared to transcripts isolated directly from the yeast in CSF ("in vivo" samples). (D) Levels of persistence of the WT, *acs1*Δ, *snf1*Δ, or *snf1*Δ *SNF1* mutant strains of *C. neoformans* were compared by measuring the number of CFU of each strain isolated from the CSF of male NZW rabbits over time as described previously (24, 42). Rabbits were infected with 10^8 CFU of either the WT, the *acs1*Δ, the *snf1*Δ, or the *snf1*Δ *SNF1* strain, and fungal burden was assessed over the course of 2 weeks as described in Materials and Methods. Missing data for the *snf1*Δ *SNF1* strain on day 13 reflects the mortality of all these rabbits before day 13. Statistical differences were assessed by an ANOVA comparison of the graphed lines using the fit model process in JMP version 8 (SAS Institute, Inc., Cary, NC) (*, $P < 0.0001$).

Fig. S2 in the supplemental material). Growth rate on lactate as measured by culture absorbance was comparable to that of the wild type (WT). The *pyk1*Δ mutant showed no defects in capsule or melanin production under inducing conditions and normal growth at 37°C, and urease activity was similar to that of the WT (data not shown). Thus, the deletion of *PYK1* had no apparent effects on the classical virulence phenotypes.

The *pyk1*Δ mutant did exhibit severely decreased persistence in the rabbit CSF model (Fig. 2A). Its inability to survive in this host microenvironment was profound. Since the *pyk1*Δ mutation restricts carbon utilization to nonpreferred carbon sources like lactate and/or acetate, and since utilization of nonpreferred carbon sources is restricted in the presence of glucose by CCR, we sought to alleviate the requirement of using lactate as a sole carbon substrate while allowing lactate use for energy production in the TCA cycle by impairing CCR. In fungi, two models exist for global regulation of carbon utilization. For molds such as *Aspergillus nidulans*, the Mig1p transcription factor homolog CreA is responsible for repressing the utilization of nonpreferred carbon sources in the presence of glucose (29). This is different from what was observed for S. *cerevisiae*, where CCR is regulated by three discrete mechanisms active at different concentrations of glucose (30). Since CreA is the main repressor in molds and Mig1p-mediated repression is active at glucose levels near those seen in human CSF (30, 31), we deleted a putative *MIG1*-related carbon catabolite repressor homolog in both WT and *pyk1*Δ backgrounds. The identity of the *MIG1* gene was verified by real-time PCR (see Materials and Methods) because we observed repression of the key gluconeogenesis genes *FBP1* and *PCK1* in *C. neoformans* (3- and 169-fold repressed in the WT, respectively); these genes are known to be repressed by Mig1p in S. *cerevisiae*. The resulting *pyk1*Δ/*mig1*Δ mutant strain should potentially utilize lactate for energy in the presence of glucose and allow utilization of numerous glycolytic metabolites as building blocks for DNA, proteins, etc.

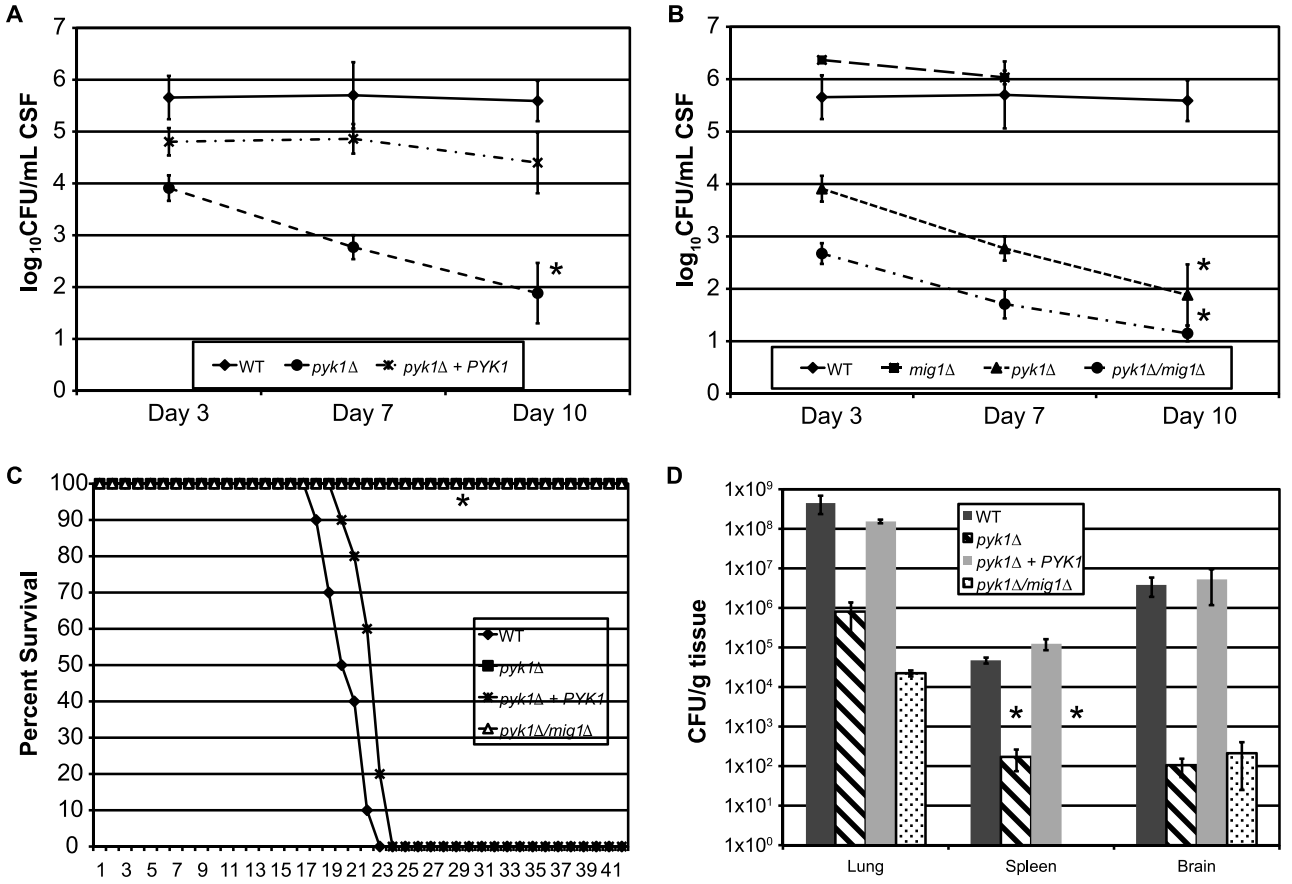

FIG 2 Uncoupling of glycolysis from oxidative phosphorylation results in complete attenuation of virulence, but not persistence, of *C. neoformans*. NZW rabbits were infected with either the WT, *pyk1*Δ, or *pyk1*Δ *PYK1* strain (A) or the WT, *mig1*Δ, *pyk1*Δ, or *pyk1*Δ/*mig1*Δ strain (B) of *C. neoformans* as described in Materials and Methods. Differences between strains were assessed by an ANOVA using the fit model process in JMP version 8 (SAS Institute, Cary, NC) (*, $P < 0.0001$). Missing data for *mig1*Δ day 10 reflects the mortality of all these rabbits before day 10. (C) A/Jcr inbred mice were infected per nasally with the WT, *pyk1*Δ, *pyk1*Δ *PYK1*, or *pyk1*Δ/*mig1*Δ strain of *C. neoformans*. The mice were observed over the course of the experiment for clinical signs correlating with eventual mortality (*, $P < 0.0001$; log rank test). (D) Fungal burden was assessed for three mice per group from the virulence study described for panel C. Organs were removed at time of death (~21 days postinfection for the WT and *pyk1*Δ *PYK1* strains; 42 days postinfection for the *pyk1*Δ and *pyk1*Δ/*mig1*Δ strains) and processed for fungal burden as described elsewhere (70). Differences in numbers of CFU between each mutant strain and the WT for each organ were assessed using Student's *t* test (*, $P = 0.01$). Missing data for *pyk1*Δ *mig1*Δ spleen counts reflect an absence of CFU detected in this sample.

Interestingly, the *pyk1*Δ/*mig1*Δ mutant showed further decreased persistence in the rabbit CSF model compared to the *pyk1*Δ mutant strain (Fig. 2B), and this was not a CNS-site-specific finding, since both mutants exhibited severely attenuated virulence in the murine inhalation model (Fig. 2C). To further define the mechanism of the attenuated virulence in the murine inhalation model, fungal viability as measured by tissue colony counts was obtained from lungs, spleen, and brain of mice at time of death (or the end of the experiment for the mutant-infected mice). As shown in Fig. 2D, despite no apparent evidence of host disease, substantial numbers of viable cells of both the *pyk1*Δ and *pyk1*Δ/*mig1*Δ mutants were recovered from mouse organs after 42 days postinfection. Additionally, colony counts were lower for the *pyk1*Δ/*mig1*Δ mutant strain than for the *pyk1*Δ strain. Clearly, these mutants can survive for long periods of time in the murine host without producing disease yet are unable to do so in the rabbit CSF model where they do not produce disease and are eliminated from the site of infection.

Hexose kinase activity is important for *C. neoformans* pathogenesis. To more directly assess the mechanistic effect of glucose utilization on virulence of *C. neoformans* in the host, we blocked glycolysis at the entry point of glucose into the glycolysis pathway via the concurrent deletion of the putative hexose kinase homologs *HXK1* and *HXK2*. Unlike the model yeast *S. cerevisiae*, which has three hexose kinase genes, *C. neoformans* possesses two putative hexose kinase genes, as observed in A. *nidulans* (22, 32). Whereas the single hexose kinase mutants and the WT strain were fully virulent, concurrent deletion of both putative hexose kinase genes by the creation of a double knockout mutation in C. *neoformans* significantly decreased fungal persistence in the rabbit CSF model (Fig. 3A). The *hxk1*Δ/*hxk2*Δ mutant also showed profoundly attenuated virulence in the murine inhalation model of cryptococcosis, compared to the single mutants and the WT strain (Fig. 3B), without apparent defects in capsule production (data not shown). Surprisingly, subsequent analysis of the fungal census from various mouse organs obtained from the murine inhalation study revealed that both the single and the double mutant strains were recovered from mice at the time of death in similar numbers, yet the speeds of disease progression were dramatically different (i.e., at the end of the experiment [21 days postinfection for the

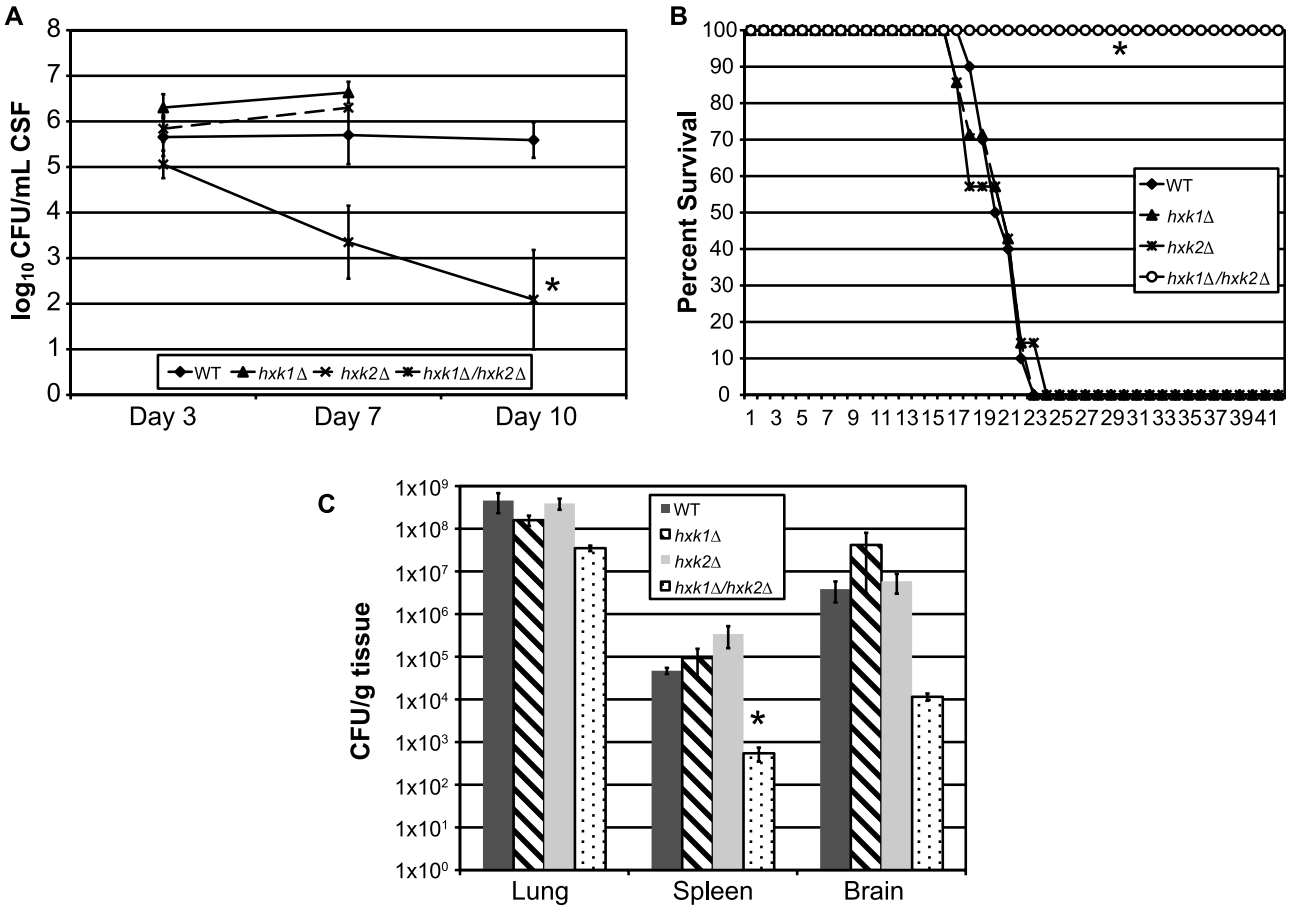

FIG 3 Glucose utilization via hexose kinase is required for virulence but not persistence of *C. neoformans*. (A) NZW rabbits were infected with either the WT, the *hxk1*Δ, the *hxk2*Δ, or the *hxk1*Δ/*hxk2*Δ strain of *C. neoformans* as described in Materials and Methods. Differences between strains were assessed by an ANOVA using the fit model process in JMP version 8 (SAS Institute, Inc., Cary, NC) (*, $P = 0.001$). Missing data for the *hxk1*Δ and *hxk2*Δ strains for day 10 reflect the mortality of all these rabbits before day 10. (B) A/Jcr inbred mice were infected per nasally with the WT, *hxk1*Δ, *hxk2*Δ, or *hxk1*Δ/*hxk2*Δ strain of *C. neoformans*. The mice were observed over the course of the experiment for clinical signs correlating with eventual mortality (*, $P < 0.0002$; log rank test). (C) Fungal burden was assessed for three mice per group from the virulence study described for panel B. Organs were removed at the time of death (~21 days postinfection for the WT, *hxk1*Δ, and *hxk2*Δ strains; 42 days postinfection for the *hxk1*Δ/*hxk2*Δ strain) and processed for fungal burden as described elsewhere (70). Differences in numbers of CFU between each mutant strain and the WT for each organ were assessed using Student's *t* test (*, $P = 0.01$).

*hxk1*Δ and *hxk2*Δ mutants and 42 days postinfection for the *hxk1*Δ/*hxk2*Δ mutant]) (Fig. 3C).

Given the results of the *pyk1*Δ, *pyk1*Δ/*mig1*Δ, and *hxk1*Δ/*hxk2*Δ mutants in both animal models, we elected to study the long-term effects of these mutations on yeast survival in the murine inhalation model. Mice were infected with either the WT, the *pyk1*Δ, the *pyk1*Δ/*mig1*Δ, or the *hxk1*Δ/*hxk2*Δ strain and evaluated every 3 weeks for fungal burden in both brain and lung tissues. These mutants did not successfully establish a persistent infection in the brains of these mice during the duration of the study (data not shown). However, all 3 mutants successfully colonized the lungs (Fig. 4A), and evaluation of these mice for signs of morbidity revealed differences in virulence in this model not previously observed (Fig. 4B). Surprisingly, the *hxk1*Δ/*hxk2*Δ mutant was shown to be virulent and caused mortality in these mice after 6 weeks postinfection. The *pyk1* mutant also displayed some virulence capacity, although by 21 weeks postinfection, this strain was cleared by the mice. Interestingly, impairment of CCR in the *pyk1*Δ background via the concurrent deletion of *MIG1* completely abolished mortality compared to the level for the *pyk1*Δ single mutant and conferred prolonged persistence of the yeast in the lung (Fig. 4). Despite their common effects on glucose assimilation via glycolysis, either at the point of entry of glucose into glycolysis (*hxk1*Δ/*hxk2*Δ) or directly before entry of pyruvate into the TCA cycle (*pyk1*Δ), virulence is severely affected, yet the final dispositions of these glycolysis mutants within the host are clearly different.

***C. neoformans* glycolysis mutants exhibit different host stress susceptibilities during infection.** To understand the mechanism(s) surrounding the impact of glycolytic interruptions on host outcomes, and since glycolysis provides metabolites for energy production via oxidative phosphorylation, we quantified ATP production in the *pyk1*Δ mutants following exposure to human CSF *in vitro* to determine a possible link between energy production and virulence in the subarachnoid space. Following 1 h of CSF exposure, the *pyk1*Δ mutant possessed equal amounts of ATP per μg protein compared to the WT (Fig. 5A). However, after 24 h of CSF exposure, the *pyk1*Δ mutant exhibited significantly less ATP than the WT. Removing carbon catabolite repression in the *pyk1*Δ background (i.e., *pyk1*Δ/*mig1*Δ) did not completely alleviate this energy production deficiency in *ex vivo* human CSF (Fig. 5A). To further differentiate whether this defi-

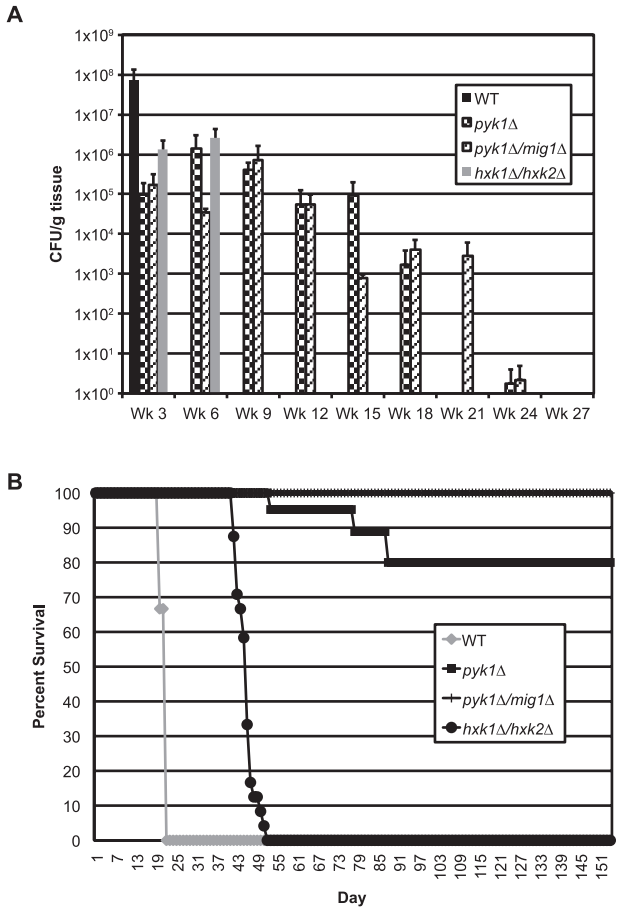

FIG 4 Pyruvate kinase mutants exhibit enhanced persistence in the lung without disease production. A/Jcr inbred mice were infected per nasally with the WT, *pyk1*Δ, *pyk1*Δ/*mig1*Δ, or *hxk1*Δ/*hxk2*Δ strain of *C. neoformans* in order to assess the persistence of these strains *in vivo*. (A) Fungal burden in lung tissues was assessed for three mice per strain every 3 weeks following infection as described elsewhere (70). Brain tissues from these mice showed no fungal burden over the course of the experiment. (B) The mice in the fungal burden assay were also observed over the course of the experiment for clinical signs correlating with eventual mortality (≥15% loss of body weight, lack of grooming, etc.). The survival of mice not sampled at the predetermined endpoints was assessed for similarity to the WT level. All mutant strains showed statistically significant differences from the WT ($P < 0.0001$; log rank test).

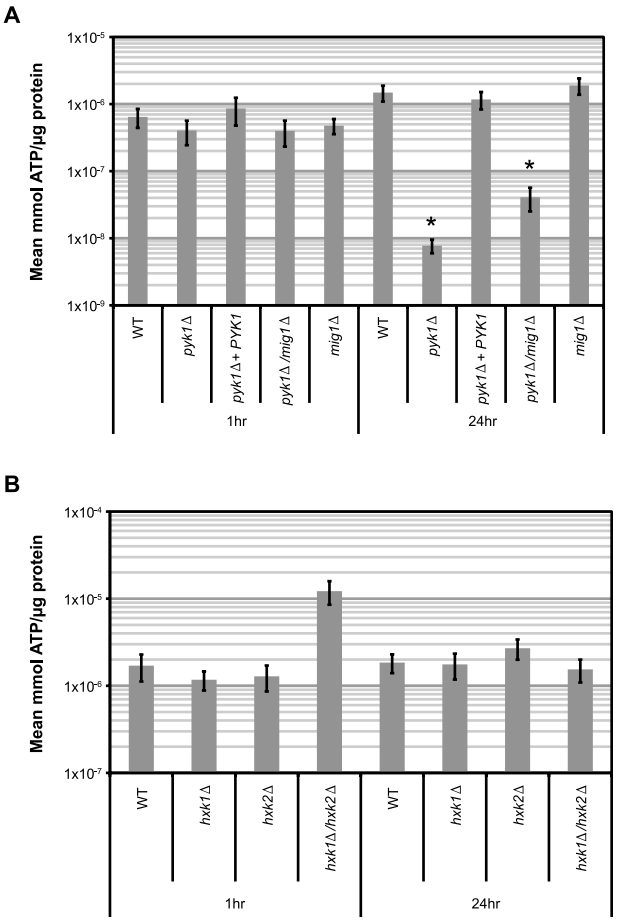

FIG 5 Mutations blocking glucose utilization produce varied effects on ATP production in *ex vivo* human CSF. WT and mutant strains of *C. neoformans* were grown in YPL shake culture at 37°C to saturation, then centrifuged, washed with sterile PBS, and resuspended in filter-sterilized pooled human CSF. These CSF shake cultures were then incubated at 37°C, with 15-ml aliquots removed at 1 h and 24 h, and processed as described elsewhere (67). (A) Measurement of ATP levels in the WT, *pyk1*Δ, *pyk1*Δ *PYK1*, *pyk1*Δ/*mig1*Δ, and *mig1*Δ strains following exposure to *ex vivo* CSF for 1 h or 24 h. Differences between mutant strains and the WT at each time point were compared using Student's *t* test (*, $P < 0.005$). (B) Measurement of ATP levels in the WT, *hxk1*Δ, *hxk2*Δ, and *hxk1*Δ/*hxk2*Δ strains following exposure to *ex vivo* CSF for 1 h or 24 h. Differences between mutant strains and the WT at each time point were compared using Student's *t* test ($\alpha = 0.05$).

ciency was due specifically to the loss of glucose utilization or more generally to the blocked entry of numerous carbon metabolites into oxidative phosphorylation, we also examined ATP production in the hexose kinase mutants (Fig. 5B). The *hxk1*Δ/*hxk2*Δ mutant is completely unable to grow on glucose as a sole carbon source but can utilize other carbon sources, such as glycerol or lactate (see Fig. S2 in the supplemental material). Interestingly, no statistically significant differences were observed between the hexose kinase single or double mutants and the WT, supporting the conclusion that the ATP production defect in CSF is due to the impaired ability of the *pyk1*Δ mutants to move carbon metabolites into the TCA cycle as substrates for oxidative phosphorylation.

To determine the cause of the attenuation in virulence in the *hxk1*Δ/*hxk2*Δ mutant if energy production is not an issue, we performed a macrophage-killing assay. This assay allowed us to assess the ability of strains to survive and proliferate in an intracellular environment. As shown in Fig. S3 in the supplemental material, defects at the beginning and end of glycolysis result in reduced survival within host cells. In fact, the *hxk1*Δ/*hxk2*Δ mutant is particularly susceptible to killing by macrophages, as this mutant was significantly reduced in survival compared to all other mutant strains tested in this macrophage assay. The *hxk1*Δ/*hxk2*Δ mutant result is at least somewhat explained due to this mutant's increased susceptibility to hydrogen peroxide and nitric oxide killing compared to that of the other mutant strains that show no added sensitivity compared to the WT (H_2O_2 MIC = 250 μM for the *hxk1*Δ/*hxk2*Δ mutant versus 2,000 μM for the WT; NO^- MIC = 62.5 μM for the *hxk1*Δ/*hxk2*Δ mutant versus 250 μM for the WT).

DISCUSSION

Previous studies by others investigating various carbon metabolic pathways in fungal pathogens have shown the importance that

carbon metabolism plays in fungal infection. For example, isocitrate lyase is a gateway enzyme for the glyoxylate shunt that allows for the utilization of 2-carbon compounds such as acetate and ethanol (18, 33, 34). The glyoxylate shunt has been shown to play a significant role in the virulence of numerous plant and animal pathogenic fungal species and interacts with the β-oxidation pathway for fatty acid utilization, as isocitrate lyase mutants in other fungal systems are also unable to utilize fatty acids as sole carbon sources (18, 35–38). However, these data from other fungi stand in direct contrast to observations in C. *neoformans* and *A. fumigatus*, where carbon acquisition via the glyoxylate shunt is not required for virulence (22, 24, 39, 40).

In the current study, we have further defined the carbon assimilation pathways in C. *neoformans* necessary for growth in discrete host microenvironments. We employed two different yet complementary models of *C. neoformans* virulence, the murine inhalation model and the rabbit CSF model (41, 42). The murine inhalation model corresponds closely to the mechanism of human infection, whereas the rabbit CSF model allows us to specifically probe the influence of the various carbon utilization pathways on CNS persistence. The linkage of gluconeogenesis via Pck1 (see Fig. S1 in the supplemental material) to C. *neoformans* virulence was first made using a random-insertion mutagenesis screen that identified the virulence-associated DEAD box RNA helicase gene *VAD1* by the Williamson laboratory (23). *PCK1* is regulated in part by Vad1, encodes a key enzyme for entry of 2- and 3-carbon compounds into gluconeogenesis, and is upregulated in response to low glucose levels. The *pck1*Δ deletion strain of C. *neoformans* exhibits severely attenuated virulence in a murine inhalation model of cryptococcosis (23). Using a separately constructed *pck1*Δ strain, we have shown that although the gene is highly upregulated in the low-glucose environment of the CSF, loss of *PCK1* yields no impact on persistence of *Cryptococcus* in the rabbit CSF model of cryptococcosis (Fig. 1).

Likewise, a prior study demonstrated roles for the nonpreferred carbon utilization regulatory kinase gene *SNF1* and the acetyl-CoA synthase gene *ACS1* in *C. neoformans* virulence in a murine inhalation model (21). Interestingly, these mutations either moderately affected or had no effect on persistence of *C. neoformans* in the rabbit CSF model of disease, which places different host site demands on the yeast regarding establishment of infection compared to those in the murine inhalation model (Fig. 1). These gluconeogenesis-related gene data, along with previously published data on *ICL1* (24) and *MLS1* (22), which demonstrate no defects in virulence due to lost glyoxylate-shunt function, clearly show that gluconeogenesis is not primarily utilized by *C. neoformans* to procure nonpreferred carbon (e.g., lactate, acetate, etc.) during growth in the CNS.

The obvious alternative to using gluconeogenesis for carbon acquisition in the CNS is glycolysis. Previous studies of cryptococcosis have touched on pathways linked to glycolysis but have not explicitly addressed the glycolysis pathway and its linkage to the virulence composite of C. *neoformans*. For example, the trehalose biosynthesis pathway has been studied for both *C. neoformans* and *C. gattii* (43, 44). In the most recent study, the relationship between trehalose biosynthesis and hexose kinase activity was demonstrated via the ability of individual hexose kinase deletion mutants to suppress the temperature-sensitive (ts) phenotype of the trehalose pathway mutants (43). However, the specific effect of hexose kinase deletions on the virulence composite was not addressed. Therefore, in this study we showed that hexose kinase activity for glucose utilization is critical both for virulence in the murine inhalation model of cryptococcosis and for acute persistence in the rabbit CSF model (Fig. 3 and 4).

The defined roles of hexose kinase in glucose catabolite repression and glucose metabolism (reviewed in reference 45) allowed us to begin to tease apart glucose utilization versus energy production in regard to their effect on virulence and growth of *C. neoformans* in the host. Three different mechanisms for glucose catabolite repression that are dependent on the level of extracellular glucose have been described for *S. cerevisiae*: the Mig1p-independent pathway (very low glucose), the Ras/cyclic AMP (cAMP) pathway (low glucose), and the Mig1p-dependent pathway (high glucose) (30). In the Mig1p-mediated glucose catabolite repression pathway, Hxk2p interacts with Mig1p to enter the nucleus and bind as a complex to glucose-repressible genes (reviewed in reference 45). Our data show a profound attenuation of virulence due to blocked metabolism of glucose in the *hxk1*Δ/*hxk2*Δ double mutant, in spite of adequate persistence of this mutant strain in the host (Fig. 3B and C and 4). However, ATP production in *ex vivo* CSF was unaffected by deletion of both hexose kinases (Fig. 5B). Therefore, these data suggest that in the absence of normal Hxk2/Mig1-mediated glucose repression (due to a lack of Hxk2), nonpreferred carbon sources are able to adequately sustain survival of the yeast in the host, with delayed expression of disease symptoms.

We have also demonstrated the importance of glucose metabolism to virulence by examining the role of pyruvate kinase, located at the opposite end of the glycolytic pathway from hexose kinase (see Fig. S1 in the supplemental material). In these studies, blocking glycolysis via deletion of *PYK1* again results in attenuated virulence, albeit apparently for a different reason. ATP production in the *pyk1*Δ mutant was severely impaired after only 24 h of exposure to *ex vivo* CSF (Fig. 5A); this demonstrates a mechanism for the adverse effect on persistence in the host CSF through reduction in energy formation (Fig. 2A and D). However, glucose catabolite repression is still active in the *pyk1*Δ mutant, and even though ample lactate is present in CSF, it may not be available for use. Therefore, we attempted to alleviate Mig1-mediated glucose catabolite repression through the deletion of the candidate *MIG1* gene in the *pyk1*Δ background and were able to partially restore ATP production (Fig. 5A). Interestingly, persistence in the host CSF was made even worse than that obtained with the single *pyk1*Δ mutant (Fig. 2B and D). In other fungal systems, deletion of *MIG1* (or its homolog *creA*) results in reduced/altered growth (46–48). It is possible that loss of Mig1-mediated repression in the *pyk1*Δ/*mig1*Δ mutant further impairs growth by allowing many carbon metabolic pathways to be activated due to the availability of all present carbon sources in the host. The putative activation of these metabolic pathways may simply outstrip the ability of available lactate to provide adequate ATP via oxidative phosphorylation, due to the block at the step of Pyk1. Alternatively, loss of Mig1-mediated repression may lead to increased activity of alternate glucose repression pathways, as has been described for deletion of *HXK2* in budding yeast (49), or other pleiotropic effects, as has been demonstrated for *SNF1*. Additional experiments will need to be performed to address this issue.

Taken together, the *hxk1*Δ/*hxk2*Δ and *pyk1*Δ data support the hypothesis that blocks at different steps in glycolysis can result in completely different mechanisms for virulence attenuation. The

hexose kinase double mutant still possesses the ability to produce ATP (Fig. 5B), but it shows increased sensitivity to reactive oxygen species (ROS) and reduced intracellular growth likely due to blocked movement of glucose-6-phosphate into the pentose phosphate pathway (50, 51). The hexose kinase and *pyk1*Δ single mutants also exhibited decreased survival in the macrophage assay but did not demonstrate particular sensitivity to ROS or nitric oxide, suggesting that the decreased survival in macrophages may have been more closely related to the use of glucose in the media necessitated by this assay. Still, the *hxk1*Δ*/hxk2*Δ mutant did show significantly decreased survival in macrophages compared to the corresponding single mutants and displays increased sensitivity to ROS compared to all other strains in this study, suggesting that the *hxk1*Δ*/hxk2*Δ mutant phenotype *in vivo* may be at least partially due to decreased survival in macrophages. Interestingly, this increased ROS sensitivity should slow the proliferation of the organism in the host, yet our data show that it may eventually adapt and kill the host (Fig. 3C and 4B). Alternatively, blocking efficient ATP (energy) production by deletion of *PYK1* (Fig. 5A) produces a strain that does not completely die in the host but persists for long periods of time (Fig. 4). In the rabbit CSF model of acute infection, both blocks in glycolysis provide substantial challenges for the survival of the yeast in this biological fluid and the CNS site of infection (Fig. 2A and 3A).

Mechanistically, it has previously been shown that activated macrophages inhibit growth of *C. neoformans in vitro* (52). The specific mechanism of growth inhibition by macrophages was first described in regard to interactions with neoplastic tumor cells and involved the inhibition of mitochondrial oxidative phosphorylation in the neoplastic cells (53, 54), which is phenotypically similar to the effect observed in *C. neoformans*, another eukaryote. It is possible that this yeast interaction with activated macrophages in immunocompetent hosts results in dormancy of the fungus through reduction or elimination of its energy production, which is then able to reestablish infection later when host immune conditions are reduced and thus more conducive for yeast growth by eliminating the block in energy production (55). The *pyk1*Δ mutation actually mimics impaired oxidative phosphorylation, as evidenced by the decrease in ATP production observed in CSF (Fig. 5A), and further shows greatly impaired proliferation in association with an activated macrophage-like cell line (see Fig. S3 in the supplemental material). These data, along with the long-term persistence data (Fig. 4), allude to the establishment of a dormant-like state in the *pyk1*Δ mutants due to disrupted oxidative phosphorylation since these cells are viable without causing disease. Therefore, we believe that the *pyk1*Δ mutants may serve as good model strains for studying the proposed yeast energy impact on dormancy of *C. neoformans*.

The impact of ATP production on persistence has implications for future antifungal development. For example, the importance of glucose metabolism on cancer growth is the subject of considerable research and is fairly well understood (25). Indeed, glycolysis inhibitors are currently in various stages of clinical trials as viable treatments for cancer (26) and may be of additional benefit in instances where anticancer drug resistance is an issue (56). Therefore, glycolysis inhibitors may provide similar benefits in the prophylaxis and treatment of fungal diseases such as cryptococcosis. The findings presented in this work suggest new targets for antifungal therapy that may help alleviate the problem of antifungal drug resistance by attacking slow-growing or dormant yeast cells.

MATERIALS AND METHODS

Strains and media. The *Cryptococcus neoformans* strains used in this study are listed in Table S1 in the supplemental material. The *C. neoformans* 44-1 and HC1 strains are clinical isolates from deidentified patients with cryptococcal meningitis and were procured from the Duke University Infectious Disease Specimen Repository. All gene deletions were performed in the *C. neoformans* H99 strain background. Strains were grown using standard yeast media as described previously (57). The 20% lactate solution used to provide a carbon source for the *pyk1*Δ mutant strains was prepared by diluting concentrated D,L-lactic acid (item no. L6661; Sigma-Aldrich, St. Louis, MO) in sterile distilled H_2O (dH_2O) and adjusting the pH of the solution to ~4.5 by adding 5.8 g/liter NaOH. Selective media contained either nourseothricin (clonNAT; 100 mg/liter; Werner BioAgents, Jena-Cospeda, Germany) or geneticin (G418; 200 mg/liter; Invitrogen Corp., Carlsbad, CA) for selection of transformants. Capsule-inducing medium (Dulbecco's modified Eagle's medium [DMEM] with or without 22 mM $NaHCO_3$ buffer, 10% NCTC 109, 10% fetal calf serum, 1% minimal essential medium [MEM] nonessential amino acid solution, 1% penicillin-streptomycin) was prepared as previously described (58), using carbon sources conducive for growth of the various mutant strains. Melanin production was visually assessed using dopamine agar (59). Urease activity was verified as previously described (60).

Gene deletions. We identified the *C. neoformans PCK1* (CNAG_04217), *PYK1* (CNAG_01820), *HXK1* (CNAG_05480), and *MIG1* (CNAG_06327) genes by searching the *C. neoformans* H99 predicted-protein database available from the Broad Institute (http://www.broadinstitute.org/annotation/genome/cryptococcus_neoformans/MultiHome.html), using a BLASTp homology search with the Pck1p, Pyk1p, Hxk1p, and Mig1p protein sequences from *S. cerevisiae*. Genes carrying *HXK2* (CNAG_03769), *ACS1*, and *SNF1* have previously been identified and are listed in Table S1 in the supplemental material. The *PCK1* and *PYK1* gene homologs are present in the *C. neoformans* genome as single copies, with 66% and 64% identity to the corresponding S. *cerevisiae* protein sequences, respectively. Hxk1 shows 35% identity to *S. cerevisiae* Hxk1p and has previously been identified (22). C. *neoformans* Mig1 exhibits 80% and 89% identity to the *S. cerevisiae* Mig1p and A. *nidulans* CreA putative DNA binding domains, respectively.

After identifying the loci of these genes in the H99 genome, we constructed PCR primers to delete the genes using established methods (see Table S2 in the supplemental material) (61). Gene deletions were verified by Southern hybridization (62), and previously unpublished gene deletion strains with altered phenotypes were complemented by reintroduction of the native gene by biolistic transformation as previously described (63). A functional role for the *MIG1* gene in the regulation of gluconeogenesis was established by comparison of transcription of putative Mig1-regulated genes (*ACS1*, *PCK1*, and *FBP1*) between the WT and *mig1*Δ strains as described below for real-time PCR.

Carbon utilization screen. The WT, *pyk1*Δ, *pyk1*Δ *PYK1*, *pyk1*Δ*/mig1*Δ, *mig1*Δ, *pck1*Δ, *hxk1*Δ, *hxk2*Δ, and *hxk1*Δ*/hxk2*Δ strains were grown to saturation in 5 ml of either yeast extract-peptone-dextrose (YPD) or yeast extract-peptone-lactate-raffinose (YPLR; 1% yeast extract, 2% peptone, 2% lactic acid, 1% raffinose) broth, counted using a hemocytometer, and diluted to 2×10^7 CFU/ml in sterile phosphate-buffered saline (PBS). A 10-fold dilution series from 2×10^7 to 2×10^4 CFU/ml was made for each strain, and 5 μl of each dilution was spotted onto yeast nitrogen base (YNB)-2% glucose, YNB-3% glycerol, and YNB-2% lactate. The plates were incubated at 30°C for 2 to 4 days and photographed.

RNA preparation. Total RNA was extracted from lyophilized cells using TRIzol reagent (Invitrogen Corp., Carlsbad, CA) and purified using a Qiagen RNeasy kit (Qiagen, Inc., Valencia, CA) in accordance with the manufacturer's instructions. RNA samples were then stored at −80°C for later analysis. For the evaluation of *PCK1* expression from anonymous human samples, RNA was extracted from either fresh (*in vivo*) or subcultured (*in vitro*) harvested cells.

Real-time PCR. cDNA was prepared from RNA purified as described above, using a RETROscript kit (Applied Biosystems/Ambion, Austin,

TX). Real-time PCR was performed on the prepared cDNA as previously described (64), using primers listed in Table S1 in the supplemental material. Transcript amplification for *PCK1* from each strain and condition was normalized to the amplification of the constitutively expressed *GPD1* gene (65). For the *ex vivo* CSF and *in vivo* rabbit expression assays, changes in transcript levels were calculated relative to the expression of *PCK1* in the WT grown in YPD at 37°C in shake culture.

To verify the identity of the *MIG1* gene, the WT and *mig1*Δ strains were grown in 50 ml YPD shake culture at 30°C overnight, washed once with sterile dH_2O, and resuspended in fresh YPD the following day for 1 h at 30°C. Following this incubation, the cultures were centrifuged, and the cell pellets were frozen at −80°C for RNA preparation as described above. The transcription levels of *ACS1*, *FBP1*, and *PCK1* were normalized to the level for the constitutively expressed *GPD1* gene in both strains. Differences in expression (*n*-fold) were calculated using the Bio-Rad iCycler software system, which utilizes the comparative cycle threshold statistical methods as previously described (66).

Measurement of ATP levels. Cellular ATP levels were measured as previously described (67), following *in vitro* CSF exposure. Briefly, fresh colonies of the WT, *pyk1*Δ, *pyk1*Δ *PYK1*, *pyk1*Δ/*mig1*Δ, *mig1*Δ, *hxk1*Δ, *hxk2*Δ, and *hxk1*Δ/*hxk2*Δ strains were grown in 30 ml of YPL broth to saturation at 37°C with shaking. The cultures were centrifuged at 3,000 rpm for 5 min, washed once with PBS, resuspended in 30 ml of filter-sterilized pooled human CSF, and incubated at 37°C with shaking. A 15-ml aliquot of each culture was removed after 1 h and 24 h and processed as follows: 10 ml was centrifuged and washed once with PBS, and the pellet was stored at −80°C; 5 ml was centrifuged and washed once with PBS, and the pellet was stored overnight at −80°C in screw-cap 2-ml tubes for analysis in the ATP assay. Pellets for ATP analysis were resuspended in 1 ml of 50 mM HEPES (pH 7.7) and disrupted using a Mini BeadBeater-16 (BioSpec Products, Inc., Bartlesville, OK) with 6.3-mm stainless steel beads. Samples were disrupted using one 45-s pulse and kept on ice before and after disruption. The disrupted samples were centrifuged at 5,000 rpm at 4°C for 10 min, and the supernatants were collected to determine ATP concentrations using an ATP bioluminescence assay kit (Sigma-Aldrich, St. Louis, MO). Soluble-protein concentrations were measured for an aliquot of the supernatant from each sample using the Bradford assay (68). ATP concentrations were normalized for direct comparison using soluble-protein concentrations for each sample. The mean measurements for three separate experiments are reported.

***In vivo* virulence experiments.** Virulence of the *C. neoformans* strains was assessed using both a murine inhalation model and a rabbit CSF model of cryptococcosis as previously described (42, 69). For the murine inhalation model, female A/Jcr mice were intranasally inoculated with 10^5 CFU/ml of each *C. neoformans* strain (10 mice per strain in survival studies; 3 mice for the WT and 27 mice per mutant strain for the fungal persistence study). For the rabbit CSF model, male New Zealand White (NZW) rabbits were treated with cortisone via daily injection and intrathecal inoculation into the subarachnoid space with 10^8 CFU of each *C. neoformans* strain (3 rabbits per group). Animals were evaluated daily for signs of morbidity and were sacrificed at predetermined clinical endpoints correlating with mortality per approval from the Duke Institutional Animal Care and Use Committee Guidelines. Differences between strains in the murine inhalation model were assessed using the log rank test in JMP version 8 (SAS Institute, Inc., Cary, NC). Differences between strains in the rabbit CSF model were determined by an analysis-of-variance (ANOVA) comparison using the Fit Model process in JMP version 8.

ACKNOWLEDGMENTS

We thank Connie Nichols and Andrew Alspaugh for thoughtful discussions of the data and its implications.

This work was supported by NIH PHS grants AI73896 and AI28388 (J.R.P.).

SUPPLEMENTAL MATERIAL

Supplemental material for this article may be found at http://mbio.asm.org/lookup/suppl/doi:10.1128/mBio.00103-11/-/DCSupplemental.

Text S1, DOC file, 0.088 MB.
Figure S1, PDF file, 0.044 MB.
Figure S2, PDF file, 0.423 MB.
Figure S3, PDF file, 0.033 MB.
Table S1, DOC file, 0.073 MB.
Table S2, DOC file, 0.090 MB.

REFERENCES

1. **Casadevall A, Perfect JR.** 1998. Cryptococcus neoformans. ASM Press, Washington, DC.
2. **Park BJ, et al.** 2009. Estimation of the current global burden of cryptococcal meningitis among persons living with HIV/AIDS. AIDS **23**:525–530.
3. **Fraser JA, et al.** 2005. Same-sex mating and the origin of the Vancouver Island *Cryptococcus gattii* outbreak. Nature **437**:1360–1364.
4. **Fraser JA, Subaran RL, Nichols CB, Heitman J.** 2003. Recapitulation of the sexual cycle of the primary fungal pathogen *Cryptococcus neoformans* var. *gattii*: implications for an outbreak on Vancouver Island, Canada. Eukaryot. Cell **2**:1036–1045.
5. **Kidd S, et al.** 2004. A rare genotype of *Cryptococcus gattii* caused the cryptococcosis outbreak on Vancouver Island (British Columbia, Canada). Proc. Natl. Acad. Sci. U. S. A. **101**:17258–17263.
6. **Perfect JR, Casadevall A.** 2002. Cryptococcosis. Infect. Dis. Clin. North Am. **16**:837–874.
7. **Diamond RD, Bennett JE.** 1973. Growth of *Cryptococcus neoformans* within human macrophages *in vitro*. Infect. Immun. **7**:231–236.
8. **Feldmesser M, Kress Y, Novikoff P, Casadevall A.** 2000. *Cryptococcus neoformans* is a facultative intracellular pathogen in murine pulmonary infection. Infect. Immun. **68**:4225–4237.
9. **Feldmesser M, Tucker S, Casadevall A.** 2001. Intracellular parasitism of macrophages by *Cryptococcus neoformans*. Trends Microbiol. **9**:273–278.
10. **Levitz SM, et al.** 1999. *Cryptococcus neoformans* resides in an acidic phagolysosome of human macrophages. Infect. Immun. **67**:885–890.
11. **Ma H, Croudace JE, Lammas DA, May RC.** 2006. Expulsion of live pathogenic yeast by macrophages. Curr. Biol. **16**:2156–2160.
12. **Perfect JR.** 2006. *Cryptococcus neoformans*: a sugar-coated killer, p. 281–303. In Heitman J, Filler SG, Edwards JE, Mitchell AP (ed.), Molecular principles of fungal pathogenesis. ASM Press, Washington, DC.
13. **Buchanan KL, Murphy JW.** 1998. What makes *Cryptococcus neoformans* a pathogen? Emerg. Infect. Dis. **4**:71–83.
14. **Chayakulkeeree M, Perfect JR.** 2006. Cryptococcosis. Infect. Dis. Clin. North Am. **20**:507–544.
15. **Moyrand F, Klaproth B, Himmelreich U, Dromer F, Janbon G.** 2002. Isolation and characterization of capsule structure mutant strains of *Cryptococcus neoformans*. Mol. Microbiol. **45**:837–849.
16. **Barelle CJ, et al.** 2006. Niche-specific regulation of central metabolic pathways in a fungal pathogen. Cell. Microbiol. **8**:961–971.
17. **Lorenz MC, Bender JA, Fink GR.** 2004. Transcriptional response of *Candida albicans* upon internalization by macrophages. Eukaryot. Cell **3**:1076–1087.
18. **Lorenz MC, Fink GR.** 2001. The glyoxylate cycle is required for fungal virulence. Nature **412**:83–86.
19. **Yin Z, et al.** 2003. Glucose triggers different global responses in yeast, depending on the strength of the signal, and transiently stabilizes ribosomal protein mRNAs. Mol. Microbiol. **48**:713–724.
20. **Lee A, et al.** 2010. Survival defects of *Cryptococcus neoformans* mutants in human cerebrospinal fluid results in attenuated virulence in an experimental model of meningitis. Infect. Immun. **78**:4213–4225.
21. **Hu G, Cheng PY, Sham A, Perfect JR, Kronstad JW.** 2008. Metabolic adaptation in *Cryptococcus neoformans* during early murine pulmonary infection. Mol. Microbiol. **69**:1456–1475.
22. **Idnurm A, Giles SS, Perfect JR, Heitman J.** 2007. Peroxisome function regulates growth on glucose in the basidiomycete fungus *Cryptococcus neoformans*. Eukaryot. Cell **6**:60–72.
23. **Panepinto J, et al.** 2005. The DEAD-box RNA helicase Vad1 regulates multiple virulence-associated genes in *Cryptococcus neoformans*. J. Clin. Invest. **115**:632–641.
24. **Rude TH, Toffaletti DL, Cox GM, Perfect JR.** 2002. Relationship of the

glyoxylate pathway to the pathogenesis of *Cryptococcus neoformans*. Infect. Immun. **70**:5684–5694.
25. **Vander Heiden MG, Cantley LC, Thompson CB.** 2009. Understanding the Warburg effect: the metabolic requirements of cell proliferation. Science **324**:1029–1033.
26. **Pelicano H, Martin DS, Xu RH, Huang P.** 2006. Glycolysis inhibition for anticancer treatment. Oncogene **25**:4633–4646.
27. **Haarasilta S, Oura E.** 1975. On the activity and regulation of anaplerotic and gluconeogenetic enzymes during the growth process of Baker's yeast. The biphasic growth. Eur. J. Biochem. **52**:1–7.
28. **Yang J, et al.** 2010. Regulation of virulence factors, carbon 1 utilization and virulence by SNF1 in *Cryptococcus neoformans* JEC21 and divergent actions of SNF1 between cryptococcal strains. Fungal Genet. Biol. **47**: 994–1000.
29. **Ronne H.** 1995. Glucose repression in fungi. Trends Genet. **11**:12–17.
30. **Yin Z, Smith RJ, Brown AJ.** 1996. Multiple signalling pathways trigger the exquisite sensitivity of yeast gluconeogenic mRNAs to glucose. Mol. Microbiol. **20**:751–764.
31. **Wishart DS, et al.** 2008. The human cerebrospinal fluid metabolome. J. Chromatogr. B Anal. Technol. Biomed. Life Sci. **871**:164–173.
32. **Flipphi M, et al.** 2003. Onset of carbon catabolite repression in *Aspergillus nidulans*. Parallel involvement of hexokinase and glucokinase in sugar signaling. J. Biol. Chem. **278**:11849–11857.
33. **Fernández E, Moreno F, Rodicio R.** 1992. The *ICL1* gene from *Saccharomyces cerevisiae*. Eur. J. Biochem. **204**:983–990.
34. **Kornberg HL.** 1966. The role and control of the glyoxylate cycle in *Escherichia coli*. Biochem. J. **99**:1–11.
35. **Cánovas D, Andrianopoulos A.** 2006. Developmental regulation of the glyoxylate cycle in the human pathogen *Penicillium marneffei*. Mol. Microbiol. **62**:1725–1738.
36. **Idnurm A, Howlett BJ.** 2002. Isocitrate lyase is essential for pathogenicity of the fungus *Leptosphaeria maculans* to canola (*Brassica napus*). Eukaryot. Cell **1**:719–724.
37. **Solomon PS, Lee RC, Wilson TJ, Oliver RP.** 2004. Pathogenicity of *Stagonospora nodorum* requires malate synthase. Mol. Microbiol. **53**: 1065–1073.
38. **Wang ZY, Thornton CR, Kershaw MJ, Debao L, Talbot NJ.** 2003. The glyoxylate cycle is required for temporal regulation of virulence by the plant pathogenic fungus *Magnaporthe grisea*. Mol. Microbiol. **47**: 1601–1612.
39. **Olivas I, et al.** 2008. Ability to grow on lipids accounts for the fully virulent phenotype in neutropenic mice of *Aspergillus fumigatus* null mutants in the key glyoxylate cycle enzymes. Fungal Genet. Biol. **45**:45–60.
40. **Schöbel F, et al.** 2007. *Aspergillus fumigatus* does not require fatty acid metabolism via isocitrate lyase for development of invasive aspergillosis. Infect. Immun. **75**:1237–1244.
41. **Lim TS, Murphy JW, Cauley LK.** 1980. Host-etiological agent interactions in intranasally and intraperitoneally induced cryptococcosis in mice. Infect. Immun. **29**:633–641.
42. **Perfect JR, Lang SD, Durack DT.** 1980. Chronic cryptococcal meningitis: a new experimental model in rabbits. Am. J. Pathol. **101**:177–194.
43. **Ngamskulrungroj P, et al.** 2009. The trehalose synthesis pathway is an integral part of the virulence composite for *Cryptococcus gattii*. Infect. Immun. **77**:4584–4596.
44. **Petzold EW, et al.** 2006. Characterization and regulation of the trehalose synthesis pathway and its importance in the pathogenicity of *Cryptococcus neoformans*. Infect. Immun. **74**:5877–5887.
45. **Gancedo JM.** 2008. The early steps of glucose signalling in yeast. FEMS Microbiol. Rev. **32**:673–704.
46. **Breslow DK, et al.** 2008. A comprehensive strategy enabling high-resolution functional analysis of the yeast genome. Nat. Methods **5**:711–718.
47. **David H, Krogh AM, Roca C, Akesson M, Nielsen J.** 2005. CreA influences the metabolic fluxes of *Aspergillus nidulans* during growth on glucose and xylose. Microbiology (Reading, Engl.) **151**:2209–2221.
48. **Shroff RA, O'Connor SM, Hynes MJ, Lockington RA, Kelly JM.** 1997. Null alleles of creA, the regulator of carbon catabolite repression in *Aspergillus nidulans*. Fungal Genet. Biol. **22**:28–38.
49. **Kümmel A, et al.** 2010. Differential glucose repression in common yeast strains in response to HXK2 deletion. FEMS Yeast Res. **10**:322–332.
50. **Brown SM, Upadhya R, Shoemaker JD, Lodge JK.** 2010. Isocitrate dehydrogenase is important for nitrosative stress resistance in *Cryptococcus neoformans*, but oxidative stress is not dependent on glucose-6-phosphate dehydrogenase. Eukaryot. Cell **9**:971–980.
51. **Juhnke H, Krems B, Kötter P, Entian KD.** 1996. Mutants that show increased sensitivity to hydrogen peroxide reveal an important role for the pentose phosphate pathway in protection of yeast against oxidative stress. Mol. Gen. Genet. **252**:456–464.
52. **Granger DL, Perfect JR, Durack DT.** 1986. Macrophage-mediated fungistasis in vitro: requirements for intracellular and extracellular cytotoxicity. J. Immunol. **136**:672–680.
53. **Granger DL, Lehninger AL.** 1982. Sites of inhibition of mitochondrial electron transport in macrophage-injured neoplastic cells. J. Cell Biol. **95**:527–535.
54. **Granger DL, Taintor RR, Cook JL, Hibbs JB.** 1980. Injury of neoplastic cells by murine macrophages leads to inhibition of mitochondrial respiration. J. Clin. Invest. **65**:357–370.
55. **Garcia-Hermoso D, Janbon G, Dromer F.** 1999. Epidemiological evidence for dormant *Cryptococcus neoformans* infection. J. Clin. Microbiol. **37**:3204–3209.
56. **Xu RH, et al.** 2005. Inhibition of glycolysis in cancer cells: a novel strategy to overcome drug resistance associated with mitochondrial respiratory defect and hypoxia. Cancer Res. **65**:613–621.
57. **Sherman F.** 1991. Getting started with yeast. Methods Enzymol. **194**:3–21.
58. **Alspaugh J, Perfect J, Heitman J.** 1998. *Cryptococcus neoformans* mating and virulence are regulated by the G-protein alpha subunit *GPA1* and cAMP. Genes Dev. **11**:3206–3217.
59. **Chaskes S, Tyndall RL.** 1975. Pigment production by *Cryptococcus neoformans* from para- and ortho-diphenols: effect of the nitrogen source. J. Clin. Microbiol. **1**:509–514.
60. **Price MS, Nichols CB, Alspaugh JA.** 2008. The *Cryptococcus neoformans* Rho-GDP dissociation inhibitor mediates intracellular survival and virulence. Infect. Immun. **76**:5729–5737.
61. **Davidson RC, et al.** 2002. A PCR-based strategy to generate integrative targeting alleles with large regions of homology. Microbiology **148**: 2607–2615.
62. **Southern EM.** 1975. Detection of specific sequences among DNA fragments separated by gel electrophoresis. J. Mol. Biol. **98**:503–517.
63. **Toffaletti DL, Rude TH, Johnston SA, Durack DT, Perfect JR.** 1993. Gene transfer in *Cryptococcus neoformans* by use of biolistic delivery of DNA. J. Bacteriol. **175**:1405–1411.
64. **Cramer KL, Gerrald QD, Nichols CB, Price MS, Alspaugh JA.** 2006. Transcription factor Nrg1 mediates capsule formation, stress response, and pathogenesis in *Cryptococcus neoformans*. Eukaryot. Cell **5**:1147–1156.
65. **Varma A, Kwon-Chung KJ.** 1999. Characterization of the glyceraldehyde-3-phosphate dehydrogenase gene [correction of glyceraldehyde-3-phosphate gene] and the use of its promoter for heterologous expression in *Cryptococcus neoformans*, a human pathogen. Gene **232**:155–163.
66. **Vandesompele J, et al.** 2002. Accurate normalization of real-time quantitative RT-PCR data by geometric averaging of multiple internal control genes. Genome Biol. **3**:RESEARCH0034.
67. **Garcia J, et al.** 2008. Mathematical modeling of pathogenicity of *Cryptococcus neoformans*. Mol. Syst. Biol. **4**:183.
68. **Bradford MM.** 1976. A rapid and sensitive method for the quantitation of microgram quantities of protein utilizing the principle of protein-dye binding. Anal. Biochem. **72**:248–254.
69. **Cox GM, Mukherjee J, Cole GT, Casadevall A, Perfect JR.** 2000. Urease as a virulence factor in experimental cryptococcosis. Infect. Immun. **68**: 443–448.
70. **Nielsen K, et al.** 2005. *Cryptococcus neoformans* {alpha} strains preferentially disseminate to the central nervous system during coinfection. Infect. Immun. **73**:4922–4933.